JOURNAL OF FUEL CHEMISTRY AND TECHNOLOGY
Volume 49, Issue 10, Oct 2021
Online English edition of the Chinese language journal

Available online at www.sciencedirect.com
ScienceDirect

Cite this article as: J Fuel Chem Technol, 2021, 49(10), 1540−1548

RESEARCH PAPER

Addition of bismuth to Pt and Pd for electric power generation with selective cogeneration of acetate from ethanol in a fuel cell type reactor

Lima F. S., Fontes E. H., Nandenha J., de Souza R.F.B., Neto A.O.*

Instituto de Pesquisas Energéticas e Nucleares, IPEN/CNEN-SP, CEP 05508-900 São Paulo, SP, Brazil

Abstract: Pt/C, PtBi(95:5)/C, Pd/C, and PdBi(95:5)/C were synthesized by the sodium borohydride reducing method to produce metal nanoparticles with advanced electronic properties to enhance the ethanol oxidation reaction (EOR) mechanism. The Transmission Electron Microscopy (TEM) images and X-ray photoelectron spectroscopy (XPS) showed that a small Bi content does not affect the nanoparticle size PdBi/C; in contrast, it does affect the PtBi ones. The X-ray diffraction analysis revealed a lattice parameter modification by Bi dope in Pt crystalline structure. Furthermore, the ATR-FTIR results indicated the suppression of carbonate formation and increment in acetate production. The results of polarization and power density curves on DEFC, the material PtBi/C presented the more high power density, almost six times bigger than Pt/C. PtBi/C also has the highest current density (44 mW/cm^2) and the lowest onset potential (−0.6 V) in linear sweep voltammetry experiments. It also has the highest final current density in current-time experiments. Hence, PtBi/C is a very promising electrocatalyst for DEFC.

Keywords: ethanol oxidation reaction; bismuth effect; co-generation of power and chemicals

Direct ethanol fuel cell (DEFC) is a promising power source studied in the last decades due to its non-toxicity, high energy efficiency, simple production from biomass fermentation, and ease of storage and transport[1–3]. However, one of the significant drawbacks of DEFC is the difficulty to cleave the ethanol C–C bond[4–6].

Those authors assign the breaking of the C–C bond, the adsorption of alcohol in multiple catalytic sites[7,8], the strongly adsorbed CO and CH_3 groups[9], with the small activity of fuel cells. Some Pt group metal catalysts can activate water at specifics potentials, overcoming the small activity mentioned above[10,11]. The activation of water in smaller potentials generates superficial oxyhydroxide species that can react with the adsorbed alcohol even linearly and lead to breaking the C–C bond[12].

Even the maximum energy efficiency of a fuel cell is linked to its fuel's complete oxidation, obtained with materials containing Rh; for example, however, they do not show significant current increases comparing to pure Pt or Pd[13–15]. Souza et al[12] working with PtSn/C + Ce/C showed that the catalytic layers that converted most ethanol to CO_2 were the ones that had less electrical current, the materials which generated more electric current; therefore, power in the cell were those whose main product was acetaldehyde and acetic acid.

Under an alkaline medium, the alcohol oxidation reactions are faster than in an acidic one, together with the fact that Pd is also more active than Pt[16]. To avoid CO poisoning and to favor the C–C ethanol bond's cleavage, the crystal structures of Pt and Pd will be modified by other element atoms[16–21] in an attempt to increase the EOR in the alkaline medium[17]. Bismuth atoms have already been studied for Pt-based materials in the alkaline medium in high relative atomic concentration (> 10%). Tusi et al[17,19,22] explained that alloy PdBi has a superior activity for EOR due to Bi's electronic effect with Pd, and Kouamé et al[18] reported that Bi and Pt have a robust electronic interaction despite the non-alloy configuration.

Ning and et al[23], justified the increase in the activity of catalysts with the addition of Bi to the geometric effect on the surface of the Pt. The bismuth act inhibiting the training and adsorption of intermediate species due to generation of bio species (OH). Neto et al[19], verified the activity of PdBi/C for oxidation of ethanol in alkaline medium reported characteristics similar to Ning et al[23]. Cai et al[24] agree that the incorporation of Bi modifies the electronic properties of

Received: 18-Mar-2021; Revised: 13-Jul-2021.
Foundation items: Supported by CAPES, FAPESP (2017/11937-4) and CNPq (302709/2020-7).
*Corresponding author. E-mail: aolivei@ipen.br.
DOI: 10.1016/S1872-5813(21)60141-X.

the noble metal, and consequently results in a material with greater activity and tolerance to the poisoning by carbon monoxide in relation to electrocatalysts of Pt/C and Pd/C.

On the other hand, the catalysts that lead to ethanol's oxidation by an incomplete route present more significant electrical currents, C2 products are not strongly adsorbed, and they also could have some value-added regarding to the alcohol itself. It is worth emphasizing that the use of fuel cells for the co-generation of energy and chemicals is showing promise for the conversion of several molecules, in milder conditions than conventional processes, in addition to the advantage of occurring in a single step and a flux system[25–30]. In this context, we studied the doping of bismuth in platinum and palladium for ethanol's oxidation reaction to obtain energy and products.

1 Methods

The sodium borohydride reduction process[1,31,32] prepared the carbon Vulcan XC-72 (Cabot) metal nanoparticles Pt/C, Pd/C, PtBi/C, and PdBi/C (20% mass ratio). The metal precursors salt $H_2PtCl_6{\cdot}6H_2O$ and $Pd(NO_3)_2{\cdot}2H_2O$ were purchased from Aldrich, and $Bi(NO_3)_3{\cdot}5H_2O$ was purchased from Alfa Aesar. PtBi means that 95% of the metal loading consists of Pt atoms, and the same goes for PdBi. The sodium borohydride synthesis method is as follows: the metal salts were dissolved in a mixture of water/2-propanol (50/50 volume ratio), and the Vulcan XC72 support was dispersed in the solution. Then, this new solution was taken to a homogenizer for 10 min. After that, the sodium borohydride reducing agent was added swiftly under vigorous stirring under ambient temperature and pressure. Finally, the mixture was filtered, and the solid was washed with ultrapure water and dried at 70 °C for 2 h[16].

All the electrocatalysts were characterized by X-ray diffraction (XRD) using the Rigaku model Miniflex II with Cu *K*α radiation source (λ = 0.15406 nm). The diffractograms were also recorded in the range of 2θ = 20° to 90° with increments of 0.05° and a scan time of 2 s per step. All the electrocatalysts were characterized by transmission electron microscopy (TEM) using the JEOL-JEM-2100 electron microscope with a 200 kV voltage. The nanoparticle's mean diameter counting procedure was performed over 200 nanoparticles; however, the TEM images are the most representative ones[33].

X-ray photoelectron spectroscopy (XPS) measurements were carried out through a spectrometer by ThermoFisher, the K-alpha+ model. The X-ray radiation source was Al *K*α and the depth of penetration was about 5 nm and spot size was set to 400 μm, which turns out to give information about the surface composition of the electrocatalysts. The powder samples were held in a copper ribbon. The final core XPS spectra were an average of three random areas at the surface of the electrocatalysts. To characterize the metals and its oxidation states we used the most intense band corresponding to a singlet or doublet states.

The electrochemical and spectroelectrochemical experiments were carryout using Autolab PGSTAT 302 N potentiostat with or without a ATR-FTIR performed in an ATR accessory (MIRacle with a ZnSe Crystal Plate Pike®) installed on a Nicolet® 6700 FT-IR spectrometer equipped with a MCT detector cooled with liquid N_2. They were all carried out at room temperature and ambient pressure, with a three-electrode cell[21]. The working electrodes were prepared by an ultra-thin porous coating technique reported by Ramos et al[34]. These electrochemical and spectro-electrochemical experiments were carried out under alkaline media (KOH 1 mol/L) with ethanol (EtOH) 2 mol/L where it was utilized a counter electrode of Pt plate and the reference electrode was Ag/AgCl. The DEFC experiments were carried out through a unitary cell of 5 cm^2 coupled to a Autolab PGSTAT 302 N potentiostat with a current booster. The fuel cell experiments were realized in fuel cell homemade consisting of two bipolar plates with serpentine channels. The MEAS consisted of an anode and a cathode pressed into the Nafion membrane, where the anode fuel concentration was 2.0 mol/L with 3.0 mol/L of KOH, with a delivery flux of 2 mL/min. The cathode was fed by oxygen with a temperature setting of 85°C, and the DEFC temperature was set up to 100°C. The Nafion® 117 membranes were immersed in 6.0 mol/L of KOH for 48 h. The normalization procedure was performed considering the unitary cell area[33].

2 Results and discussion

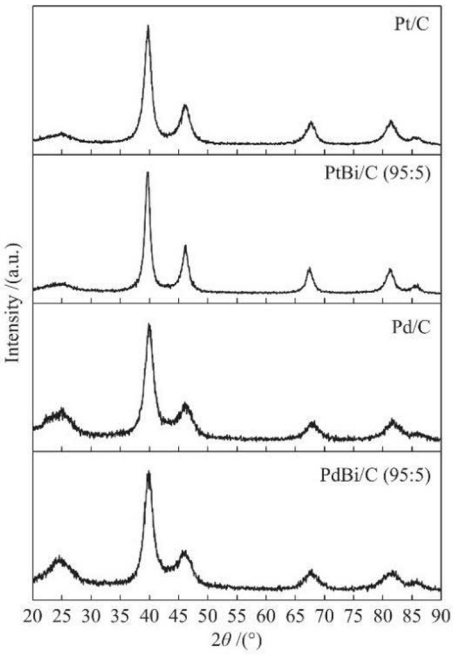

Fig. 1 XRD measurements for Pt, Pd, and Bi-material supported on carbon Vulcan XC72 for 2θ from 20° up to 90°

The X-ray diffraction patterns, in Figure 1, showed at $2\theta \approx$ 40°, 47°, 68°, 82° and 87° corresponding to the crystalline planes (111), (200), (220), (311), and (222) of the face-centered cubic (FCC) structure characteristics of Pd and Pt crystalline structure[18,22,34]. Bismuth's materials presented Bragg's peak at 68°, 82°, and 87° with small shifts to lower angles compared to Pd and Pt structures, which could be associated with a lattice parameter expansion. The lattice parameter is 0.392 nm for PdBi/C (95:5) and PtBi/C (95:5), while for Pt and Pd are respectively 0.391 and 0.389 nm respectively, in according with the literature[18,34,35].

Figure 2 shows the TEM micrographs and the nanoparticles size distribution. Note that all materials have a particle size average between 5 and 8 nm. For the platinum-based materials, bismuth's insertion increased the nanoparticle's size due to bismuth oxides[22]. However, for palladium-based materials, the nanoparticle's size remained very close to Pd/C one. After incorporating Bi onto Pd, the crystal structure stood almost the same because of the small Bi 4*f* content compared to PtBi/C, as Figure 4 shows.

Figure 3 shows the Bi 4*f*, Pd 3*d*, and Pt 4*f* core level XPS spectra. For Pt and Pd metals in all electrocatalysts is possible to identify the following oxidation states: Pd^0, Pd^{2+}, Pt^0, and Pt^{2+}[36–38]. As we should expect, those peaks position are invariant under Bi doping[18]. Nonetheless, the Bi concentration in the binary electrocatalysts was too small in the surface probe area. The XRD and XPS result strongly suggests that Bi atoms were incorporated in the Pt and Pd crystalline structures.

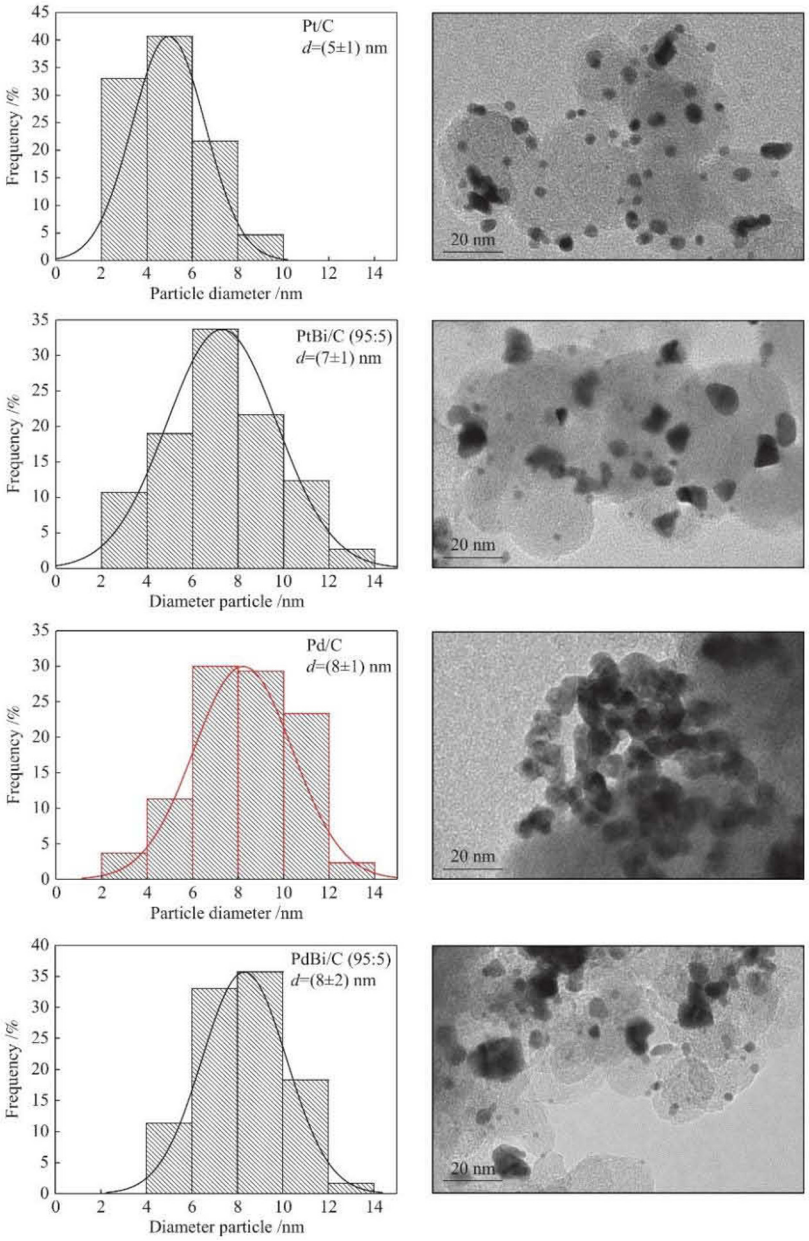

Fig. 2 Nanoparticle size distribution in its corresponding TEM images

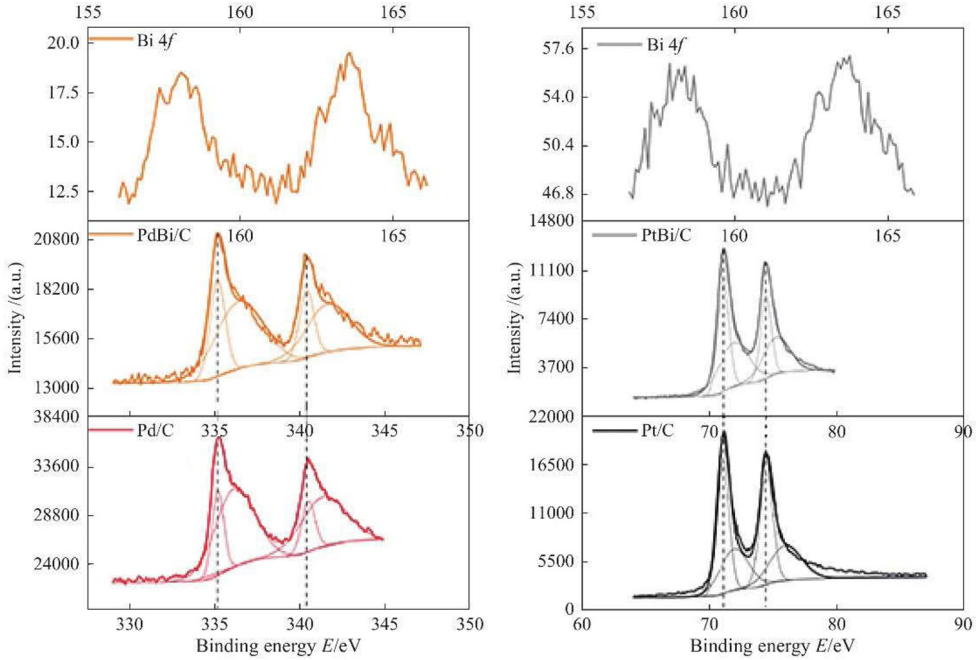

Fig. 3 XPS spectra of Bi 4*f*, Pt 4*f* and Pd 3*d* and its oxidation states, for Pt and Pd, Bi dopped materials

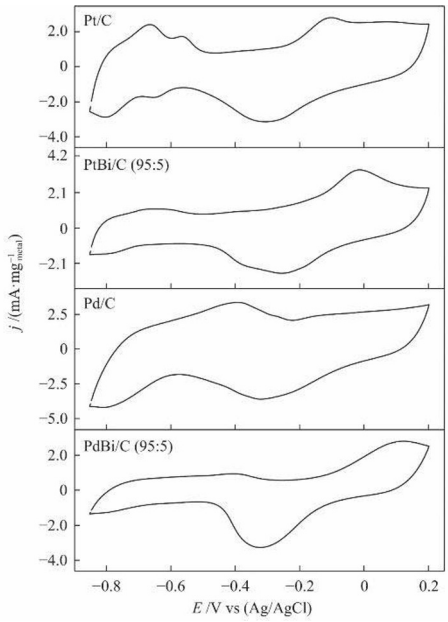

Fig. 4 Cyclic voltammetry in 1 mol/L of KOH for all electrocatalysts V = 10 mV/s

A series of cyclic voltammograms in 1 mol/L of KOH were performed to evaluate the redox process, as Figure 4 shows. The hydrogen adsorption/desorption region −0.85 at −0.4 V is suppressed by the presence of Bi atoms. Nonetheless, PdO_x/BiO_x could be related to the peak close to 0.1 V in PdBi/C, and PtO_x/BiO_x also to the peak at −0.05 V in PtBi/C. We can identify the peak associated with the reduced metal oxides (~ −0.3 V) for all electrocatalysts, following previous works[17,19].

Figure 5 shows the linear sweep voltammetry (LSV) and the current-time (CT) curves in 1.0 mol/L of KOH and 2.0 mol/L of ethanol. The LSV results (Figure 5(a)) showed that the addition of bismuth shifted the onset potential to more negative values: from ~ −0.57 V (Pt) to ~ −0.7 V (PtBi), and ~ −0.54 V (Pd) to ~ −0.6 V (PdBi). Also, the Faradaic current of ethanol oxidation has increased.

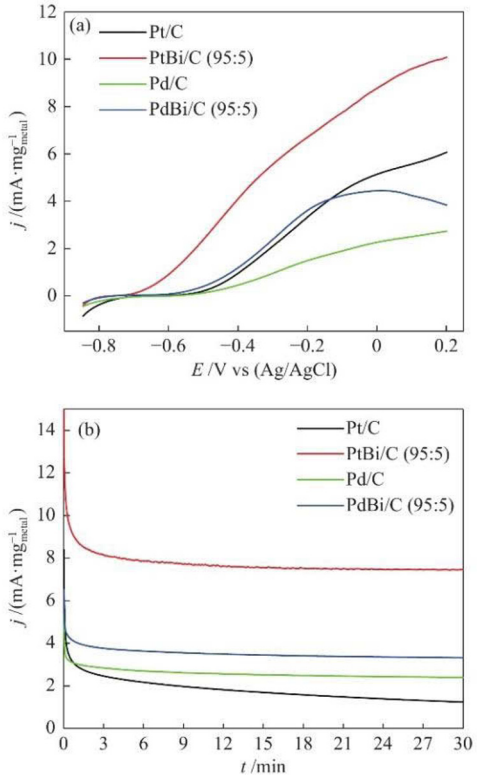

Fig. 5 (a) LSV measurement at V = 10 mV/s and (b) CT curves at −0.3V under alkaline medium 1 mol/L of KOH and ethanol 2 mol/L

In CT curves (Figure 5(b)), bismuth's effect on noble metals is also noted. It has seen an increase of 6 times in the current density for Pt and 1.5 times for Pd; moreover, the materials containing Bi showed more stability. Works that used Bi as a co-catalyst[17–19] attribute this effect to the bifunctional mechanism and the electronic interactions that alter the alcohol adsorption energy.

Figure 6 shows the main products observed through ATR-FITR experiments regarding the ethanol oxidation products: CO_2, acetate, acetaldehyde, and carbonate[39]. It is also possible to notice the symmetric stretching of CH_3COO^- (1407 cm^{-1})[40,41] and the stretching of the CO bond of CO_3^{2-} (1376 cm^{-1})[40] for all electrocatalysts. Moreover, it is possible to identify the asymmetric stretching of CO_2 (2343 cm^{-1})[1], while the C−C−O stretch of acetaldehyde (933 cm^{-1})[42] did not appear.

The same Figure 6 shows the deconvolved integration of acetate and carbonate ions to all electrocatalysts. The Bi effect suppressed the carbonate ion production in Pt and increased the acetate production, especially the palladium composition regarding the latter one. Still, considering the Bi effect, it is possible to notice that the C−C ethanol bond cleavage was ineffective. We can see it by the low rate of carbonate ions production, so we expect to mitigate the metal active sites' poisoning effect.

In Figure 7 was presented the DEFC experiments for Pd/C, PdBi/C, Pt/C, and PtBi/C electrocatalysts. The OCV measured was 0.79, 0.72, 0.82 and 0.95 V respectively for Pt/C, Pd/C, PdBi/C (95:5) and PtBi/C (95:5), it is notable that the addition of bismuth increases the cell's OCV. It is noteworthy to observe that the polarization curves and the power density curves have the same trend that CT curves 44 mW/cm^2 for PtBi/C (95:5), 22 mW/cm^2 for PdBi/C (95:5), 18 mW/cm^2 for Pd/C and 9 mW/cm^2 for Pt/C; this was expected since CT curves are also known to be a long-term stability experiment[16].

The higher power density cannot be explained only by the change in the alcohol adsorption energy. The effect of Bi on Pt/C and Pd/C should cause some enhanced electronic impact on catalysis. The oxy-hydroxyl species formed by the cell potential variation[17,19], which interacts with adsorbed ethanol, facilitates the oxidation to acetate. This process happens in one step only and very quickly. It is also noted that less power was extracted for Pt/C, which is also linked to carbonate formation that poisons the catalytic sites, which do not occur in materials containing bismuth or palladium.

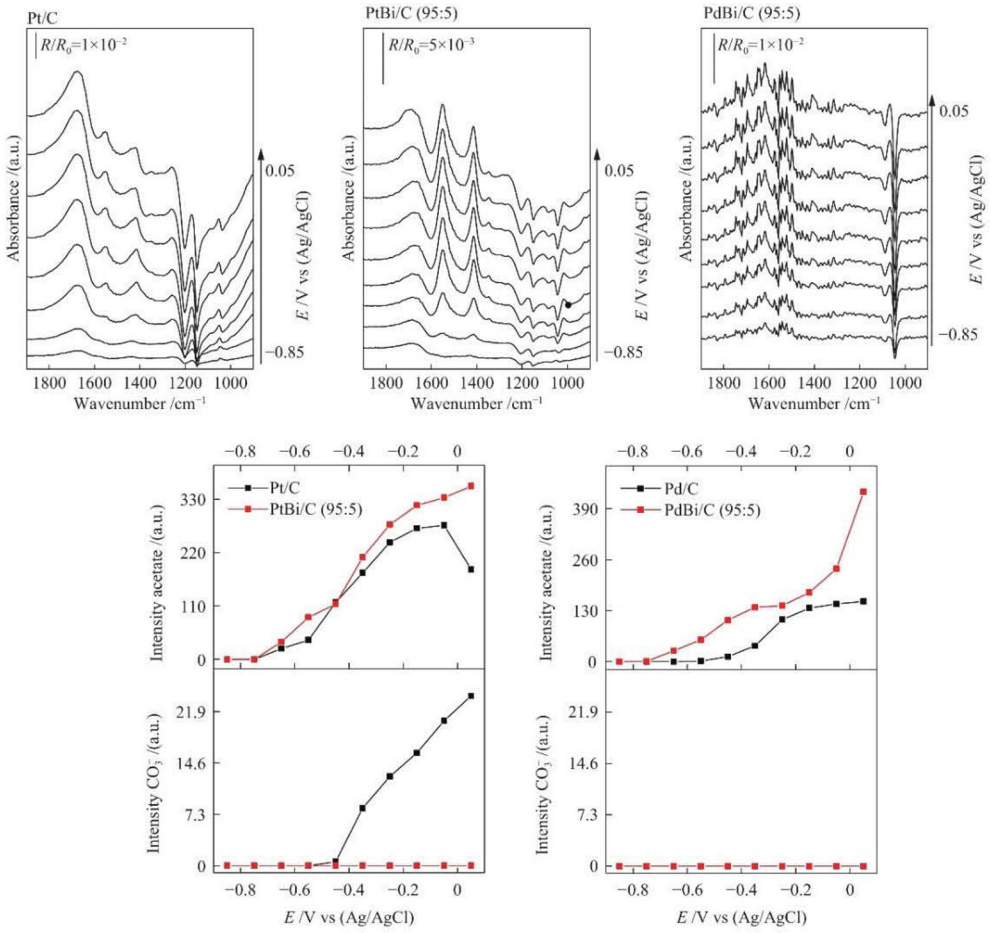

Fig. 6 ATR-FTIR spectra of ethanol 2 mol/L + KOH 1 mol/L for Pd/C, PdBi/C, Pt/C, and PtBi/C electrocatalysts the EOR products obtained through deconvolved Lorentzian bands shape, the background spectra were collected at −0.85 V, the potential step was set to 100 mV

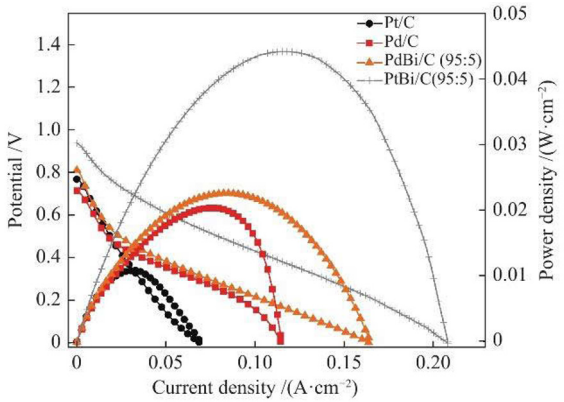

Fig. 7 DEFC experiments in ethanol 2.0 mol/L and 3.0 mol/L of KOH, with a delivery flux of 2.0 mL/min. the cathode was fed by oxygen with a temperature setting of 85°C, and the DEFC temperature was set up to 100°C

3. Conclusions

The doping of bismush in Pt and Pd proved to be promising for the co-generation of energy and acetate. The Pt/C, PtBi/C, Pd/C, and PdBi/C electrocatalysts were successfully synthesized by the sodium borohydride reduction method. They showed the FCC characteristics of Pd crystalline structure for Pd/C and PdBi/C, and the same went for Pt/C and PtBi/C. The XRD also revealed at higher angles the influence of Bi atoms in Pt crystalline structure.

The ex-situ XPS and cyclic voltammetry in 1 mol/L of KOH revealed higher oxidation states associated with these metals. The TEM micrograph showed that Pd/C has some nanoparticle aggregation, and PdBi/C has some highly ordered structure. ATR-FTIR results showed that the Bi effect suppresses the carbonate production and increases acetate production due to weak adsorption. PtBi/C presented the best electrochemical and DEFC performances due to acetate preferential formation and without carbonate ion poison.

Conflicts of interest

The authors declare no competing financial interest.

References

[1] Fontes E H, Ramos C E D, Nandenha J, Piasentin R M, Neto A O, Landers R. Structural analysis of PdRh/C and PdSn/C and its use as electrocatalysts for ethanol oxidation in alkaline medium. Int J Hydrogen Energy, 2019, 44(2): 937−951.

[2] Neto A O, Nandenha J, Assumpção M H M T, Linardi M, Spinacé E V, De Souza R F B. In situ spectroscopy studies of ethanol oxidation reaction using a single fuel cell/ATR-FTIR setup. Int J Hydrogen Energy, 2013, 38(25): 10585−10591.

[3] Almeida C V S, Almagro L E, Valério Neto E S, Coro J, Suárez M, Eguiluz K I B, Salazar-Banda G R. Polyhydroxylated fullerenes: An efficient support for Pt electrocatalysts toward ethanol oxidation. J Electroanal Chem, 2020, 878: 114663.

[4] Qian Q Y, Yang C, Zhou Y G, Yang S, Xia X H. Efficient C–C bond cleavage in ethanol electrooxidation on porous Pt catalysts. J Electroanal Chem, 2011, 660(1): 57−63.

[5] Wang F, Wang K, An C, An C, Zhang W. PtPdCu nanodendrites enable complete ethanol oxidation by enhancing CC bond cleavage. J Colloid and Interface Sci, 2020, 571: 118−125.

[6] Piwowar J, Lewera A. On the absence of a beneficial role of Rh towards CC bond cleavage during low temperature ethanol electrooxidation on PtRh nanoalloys. J Electroanal Chem, 2020, 875: 114229.

[7] Lai S C S, Koper M T M. Ethanol electro-oxidation on platinum in alkaline media. Phys Chem Chem Phy, 2009, 11(44): 10446−10456.

[8] Farias M J S, Cheuquepán W, Tanaka A A, Feliu J M. Unraveling the nature of active sites in ethanol electro-oxidation by site-specific marking of a Pt catalyst with isotope-labeled 13CO. J Phys Chem Let, 2018, 9(6): 1206−1210.

[9] Ferre-Vilaplana A, Buso-Rogero C, Feliu J M, Herrero E. Cleavage of the C–C bond in the ethanol oxidation reaction on platinum. Insight from experiments and calculations. J Phys Chem C, 2016, 120(21): 11590−11597.

[10] Markovic N M, Gasteiger H A, Ross P N, Jiang X, Villegas I, Weaver M J. Electro-oxidation mechanisms of methanol and formic acid on Pt-Ru alloy surfaces. Electrochim Acta, 1995, 40(1): 91−98.

[11] Liu J, Cao J, Huang Q, Li X, Zou Z, Yang H. Methanol oxidation on carbon-supported Pt-Ru-Ni ternary nanoparticle electrocatalysts. J Power Sources, 2008, 175(1): 159−165.

[12] De Souza R F B, Silva J C M, Assumpção M H M T, Neto A O, Santos M C. Ethanol oxidation reaction using PtSn/C + Ce/C Electrocatalysts: Aspects of ceria contribution. Electrochim Acta, 2014, 117: 292−298.

[13] Messa Moreira T F, Neto S A, Lemoine C, Kokoh K B, Morais C, Napporn T Wolivi P. Rhodium effects on Pt anode materials in a direct alkaline ethanol fuel cell. RSC Adv, 2020, 10(58): 35310−35317.

[14] Lima F H B, Profeti D, Lizcano-Valbuena W H, Ticianelli E A, Gonzalez E R. Carbon-dispersed Pt-Rh nanoparticles for ethanol electro-oxidation. Effect of the crystallite size and of temperature. J Electroanal Chem, 2008, 617(2): 121−129.

[15] Fontes E H, Da Silva S G, Spinace E V, Neto A O, De Souza R F B. In situ ATR-FTIR studies of ethanol electro-oxidation in alkaline medium on PtRh/C electrocatalyst prepared by an alcohol reduction Process. Electrocatal, 2016, 7(4): 297−304.

[16] Palma L M, Almeida T S, De Andrade A R. Comparative study of catalyst effect on ethanol electrooxidation in alkaline medium: Pt- and Pd-based catalysts containing Sn and Ru. J Electroanal Chem, 2020, 878: 114592.

[17] Tusi M M, Polanco N S O, Da Silva S G, Spinacé E V, Neto A O. The high activity of PtBi/C electrocatalysts for ethanol electro-oxidation in alkaline medium. Electrochem Commun, 2011, 13(2): 143−146.

[18] Kouamé B S R, Baranton S, Brault P, Canaff C, Chamorro-Coral W, Caillard A, De Oliveira Vigier K, Coutanceau C. Insights on the unique electro-catalytic behavior of PtBi/C materials. Electrochim Acta, 2020, 329: 135161.

[19] Neto A O, Tusi M M, De Oliveira Polanco N S, Da Silva S G, Coelho Dos Santos M, Spinacé E V. PdBi/C electrocatalysts for ethanol electro-oxidation in alkaline medium. Int J Hydrogen Energy, 2011, 36(17): 10522−10526.

[20] Du W, Mackenzie K E, Milano D F, Deskins N A, Su D, Teng X. Palladium–tin alloyed catalysts for the ethanol oxidation reaction in an alkaline medium. ACS Catal, 2012, 2(2): 287−297.

[21] Ottoni C A, Da Silva S G, De Souza R F B, Neto A O. PtAu electrocatalyst for glycerol oxidation reaction using a ATR-FTIR/single direct alkaline glycerol/air cell in situ study. Electrocatal, 2016, 7(1): 22−32.

[22] Yovanovich M, Piasentin R M, Ayoub J M S, Nandenha J, Fontes E H, De Souza R F B, Buzzo G S, Silva J C M, Spinacé E V, Assumpção M H M T, Neto A O, Da Silva S G. PtBi/C electrocatalysts for formic acid electro-oxidation in acid and alkaline electrolyte. Int J Electrochem Sci, 2015, 10(6): 4801−4811.

[23] Ning X, Zhou X, Luo J, Ma L, Xu X, Zhan L. Effects of the synthesis method and promoter content on bismuth-modified platinum catalysts in the electro-oxidation of glycerol and formic acid. ChemElectroChem, 2019, 6(6): 1870−1877.

[24] Cai J, Huang Y, Guo Y. Bi-modified Pd/C catalyst via irreversible adsorption and its catalytic activity for ethanol oxidation in alkaline medium. Electrochim Acta, 2013, 99: 22−29.

[25] Kim H J, Choi S M, Nam S H, Seo M H, Kim W B. Carbon-supported PtNi catalysts for electrooxidation of cyclohexane to benzene over polymer electrolyte fuel cells. Catal Today, 2009, 146(1/2): 9−14.

[26] Kim H J, Choi S M, Nam S H, Seo M H, Kim W B. Effect of Rh content on carbon-supported PtRh catalysts for dehydrogenative electrooxidation of cyclohexane to benzene over polymer electrolyte membrane fuel cell. Appl Catal A: Gen, 2009, 352(1/2): 145−151.

[27] Cai R, Song S, Ji B, Yang W, Xin Q, Sun G, Douvartzides S, Tsiakaras P. Benzene electro-oxidation in a PEMFC for phenol and electricity cogeneration. Appl Catal B: Environ, 2005, 61(3/4): 184−191.

[28] Bianchini C, Bambagioni V, Filippi J, Marchionni A, Vizza F, Bert P, Tampucci A. Selective oxidation of ethanol to acetic acid in highly efficient polymer electrolyte membrane-direct ethanol fuel cells. Electrochem Commun, 2009, 11(5): 1077−1080.

[29] Nandenha J, Piasentin R M, Silva L M G, Fontes E H, Neto A O, De Souza R F B. Partial oxidation of methane and generation of electricity using a PEMFC. Ionics, 2019, 25(10): 5077−5082.

[30] Buzzo G S, Rodrigues A C B, De Souza R F B, Silva J C M, Bastos E L, Spinacé E V, Neto A O, Assumpção M H M T. Synthesis of hydroquinone with co-generation of electricity from phenol aqueous solution in a proton exchange membrane fuel cell reactor. Catal Commun, 2015, 59: 113−115.

[31] Santos M C L, Nunes L C, Silva L M G, Ramos A S, Fonseca F C, De Souza R F B, Neto A O. Direct alkaline anion exchange membrane fuel cell to converting methane into methanol. ChemistrySelect, 2019, 4(39): 11430−11434.

[32] Souza F M, Nandenha J, Batista B L, Oliveira V H A, Pinheiro V S, Parreira L S, Neto A O, Santo M C. PdxNby electrocatalysts for DEFC in alkaline medium: Stability, selectivity and mechanism for EOR. Int J Hydrogen Energy, 2018, 43(9): 4505−4516.

[33] De Carmargo V F, Fontes E H, Nandenha J, De Souza R F B, Neto A O. High activity of Pt-Rh supported on C-ITO for ethanol oxidation in alkaline medium. Res Chem Intermediates, 2020, 46(2): 1555−1570.

[34] Ramos A S, Santos M C L, Godoi C M, De Queiroz L C, Nandenha J, Fontes E H, Brito W R, Machado M B, Neto A O, De Souza R F B. High CO tolerance of Pt nanoparticles synthesized by sodium borohydride in a time-domain NMR spectrometer. Int J Hydrogen Energy, 2020, 45(43): 22973−22978.

[35] Nilsson A, Pettersson L G M. Chapter 2 - adsorbate electronic structure and bonding on metal surfaces. In: Nilsson A, Pettersson LGM, Nørskov JK, editors. Chemical Bonding at Surfaces and Interfaces. Amsterdam: Elsevier; 2008: 57−142.

[36] Farnood A, Ranjbar M, Salamati H. Localized surface plasmon resonance (LSPR) detection of hydrogen gas by Pd^{2+}/Au core/shell like colloidal nanoparticles. Int J Hydrogen Energy, 2020, 45(1): 1158−1169.

[37] Liu J, Li D, Li R, Wang Y, Wang Y, Fan C. PtO/Pt^{4+}-BiOCl with enhanced photocatalytic activity: Insight into the defect-filled mechanism. Chem Eng J, 2020, 395: 123954.

[38] Motin A M, Haunold T, Bukhtiyarov A V, Bera A, Rameshan C, Rupprechter G. Surface science approach to Pt/carbon model catalysts: XPS, STM and microreactor studies. Appl Surf Sci, 2018, 440: 680−687.

[39] Antolini E, Gonzalez E R. Alkaline direct alcohol fuel cells. J Power Sources, 2010, 195(11): 3431−3450.

[40] Fang X, Wang L, Shen P K, Cui G, Bianchini C. An in situ Fourier transform infrared spectroelectrochemical study on ethanol electrooxidation on Pd in alkaline solution. J Power Sources, 2010, 195(5): 1375−1378.

[41] Zhou Z Y, Wang Q, Lin J L, Tian N, Sun S G. In situ FTIR spectroscopic studies of electrooxidation of ethanol on Pd electrode in alkaline media. Electrochim Acta, 2010, 55(27):

7995−7999.

[42] Geraldes A N, Da Silva D F, Pino E S, Da Silva J C M, De Souza R F B, Hammer P, Spinacé E V, Neto A O, Linardi M, Dos Santos M C. Ethanol electro-oxidation in an alkaline medium using Pd/C, Au/C and PdAu/C electrocatalysts prepared by electron beam irradiation. Electrochim Acta, 2013, 111: 455−465.